Jurnal Teknologi

Full Paper

# PROPER ORTHOGONAL DECOMPOSITION: A TOOL TO STUDY THE UNDERLYING PHYSICS OF TURBULENCE

Syed Mohd Yahya[a*], Syed Fahad Anwer[a], Sanjeev Sanghi[b]

[a]Mechanical Engineering Department, Aligarh Muslim University, Aligarh-202002 UP, India
[b]Applied Mechanics, Indian Institute of Technology Delhi, New Delhi-110016, India

**Article history**
Received
*16 January 2017*
Received in revised form
*14 April 2017*
Accepted
*14 August 2017*

*Corresponding author
smyahya@zhcet.ac.in

**Graphical abstract**

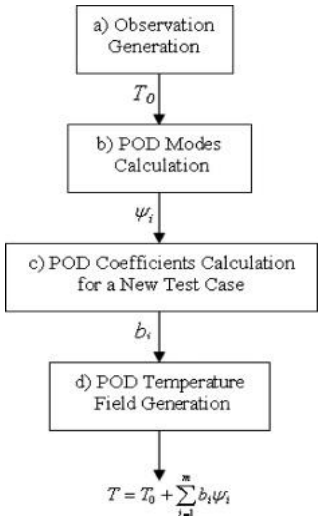


**Abstract**

Wall bounded turbulence have been investigated by many authors to understand the underlying physics, experimentally as well as numerically with different techniques and methods. Enormous studies are reported in the literature in the field of turbulence to get the insight of near wall structure in a broad spectrum of Reynolds number. To recognize the contribution of different turbulent scales in a flow a well-known technique, Proper Orthogonal decomposition (POD) is used. Dynamical behaviour of coherent structure in a turbulent channel flow submitted to high temperature gradient is investigated via proper orthogonal decomposition (POD). The turbulent data is generated using thermal large eddy simulation (TLES) of channel flow at Re = 180 for two values of temperature ratio between hot and cold wall. The POD technique is applied to fluctuating part of the velocity to study the temporal evolution of the most energetic modes. It is observed that dominant flow structures are elongated in streamwise direction which further distorted due to the interaction with bean shaped propagating modes. The plotted average energy E(t) as a function of non-dimensional time shows a constant level of fluctuating energy with one little peak at t+ = 1000, all other smaller spikes are showing constant fluctuations about mean line. This behavior at $R_\theta = 3$ quantitatively describe the role of temperature stratification which stabilizes the roll mode energy and prevent them from breakup into smaller scales thus affects the interaction process during turbulent burst event resulting in a chugging or relaminarizing phenomenon. It is observed that thermal stratification decreases the bursting rate by slowing the breaking mechanism of streamwise elongated modes to larger number of bean shaped modes which results in relaminarization of the flow near hot wall.

*Keywords*: POD, turbulent channel, energy dynamics, coherent structures, stratification



## 1.0 INTRODUCTION

Wall bounded turbulence have been investigated by many authors to understand the underlying physics, experimentally as well as numerically with different techniques and methods. It is well known that near-wall streamwise vortices play an important role in the transport mechanisms in wall turbulence, at least, at low Reynolds number flows [1–3]. Streamwise vortices and streaky structures, which are scaled with viscous wall units (see Kline *et al*. [4] ), are closely associated and regenerated through inherent near-wall mechanisms (see Hamilton *et al*. [5]). Turbulent production process in the buffer layer during ejection and sweep events refers to as the most relevant part from physical perspective. Enormous studies are reported in the literature in the field of turbulence to get the insight of near wall structure in a broad spectrum of Reynolds number. Many of them used mathematically developed model for identification of

vortical structure in a wall bounded turbulent flows [6–8]. To recognize the contribution of different turbulent scales in a flow, such a method is adopted which only extract contributing modes of the flow from the background flow in order to describe appropriately the dynamics of coherent structure. One such tecnique is the proper orthogonal decomposition (POD). The proper orthogonal decomposition or Karhunen-loève (KL) decomposition is a well-known technique for educing coherent structures of turbulent flows. Lumley [9] was the first to introduce POD in turbulence research, which is further extensively used by Sirovich [10] and Berkooz *et al*. [11]. Sirovich *et al*. [12] and Ball *et al*. [13] also applied KL decomposition to channel flow and identified various structure along with temporal behavior. A minimal channel flow analysis is performed by Webber *et al*. [14], in which they applied POD to minimal channel flow domain used by Jimènez and Moin [15], whose dynamics are known to be somewhat simpler, but reflects the representation for wall bounded turbulence obtained in larger domains. A thorough knowledge is must to know the behavior of coherent structure in wall bounded flow subjected to temperature stratification. To the best of author knowledge, POD of channel flow subjected to high temperature gradient in transverse direction has not been studied. The main aim of this work is to address the issue of coherent structure in a channel flow experiencing a high thermal field in transverse direction.

## 2.0 METHODOLOGY

In this section we describe briefly the basics of the POD procedure in three dimensions. The fluid is driven by an imposed pressure gradient in streamwise direction and flows between the two walls, which are kept at constant temperature, whereas buoyancy acts along the wall-normal direction (z). A grid size of (96×96×96) adequate for the large eddy simulation of stratified turbulent flow is used. The non-dimensional grid spacing are scaled by wall variables $z^+ = {zu_\tau}/{\vartheta}$ and $\mathrm{u_\tau} = \sqrt{\frac{\tau_w}{\rho_w}}$ where $\upsilon$ is the kinematic viscosity and $\tau_w$ is the wall shear stress. We have varied a temperature ratio $\mathrm{R_\theta} = \frac{T_h}{T_c}$ between the walls from 1.01 to 3. All simulations are performed at a constant Prandtl number $\mathrm{Pr} = 0.71$and a shear Reynolds number $\mathrm{Re_\tau} = 180$. The numerical method used for simulating channel flow in this study is taken from Yahya *et al*. [16].

Here we consider an ensemble of temporal realization or snapshots from the fluctuating flow field defined as $U^m = U(x, t_m)$ where *m=1,.....,M* corresponds to number of realizations captured numerically or experimentally. In our case the state variable $U^m$ comprises of three velocity field and one thermal field given as $U^m = (U^1, U^2, U^3, U^4)$ where$U^1 = u'$, $U^2 = v'$, $U^3 = w'$, $U^4 = \theta'$ defined at each point. The KL basis functions $\phi$ are taken to be vector function with four components at each point $(\phi^1, \phi^2, \phi^3, \phi^4)$ represnting three velocities and one thermal field. The vector space *D* in which the decomposition to be performed has an inner product defined as $(f, g) = \int (f_1 g_1 + f_2 g_2 + f_3 g_3 + \gamma f_4 g_4) dA$. Where $\gamma$ is the scaling factor which is mandatory to incorporate as to balance the energies between velocity and temperature fluctuations in order to capture the most energetic POD basis from both the fields in a unified way (see Lumley & Poje [17]). They have shown a proper value $\gamma$ of that maximizes the average of the square of the projection of the data onto the basis function $\phi$. The POD basis function $\phi$ is governed by the Fredholm integral equation of first kind or eigenvalue problem as $\oint R_{ij}(x, x')\phi_j(x')dA = \lambda\phi_i(x), \quad (i, j) \in 1,4.$ Where $R_{ij}(x, x') =< U_i(x, t_m)U_j(x', t_m) >$ is a two point state variable correlation tensor. The eigenvalue problem above yields a countably infinite orthogonal set of eigenfunctions $\phi_i^m(x_j)$ and correspondingly a real positive eigenvalue $\lambda_m$ (see Berkooz *et al*. [11]). This basis function is utilised in reconstruction of modal decomposition of the flow field as,

$$U(x, t_m) = \sum_m a^m(t_m)\phi^m(x). \qquad (1)$$

After obtaining eigenfunctions, they are normalised in a manner such that$(\phi_m, \phi_m) = 1$, and the temporal or random coefficient then can be found as $a^m(t_m) = (U, \phi^m)$.The contribution of each mode to the total energy in an average sense is given by

$$E = \langle U, U \rangle = \sum_m \sum_n (a^m a^n)(\phi^m, \phi^n) = \sum \lambda^m \qquad (2)$$

If the obtained non-negative eigenvalues are sorted in a decreasing order such that $\lambda^1 > \lambda^2 > \lambda^3 \ldots\ldots$,the sequence at the right of eq.(1) converges more rapidly than with any other KL basis. We have used the truncation criterion proposed by Dean & Sirovich[18] for the infinite sequence in eq.(1) to confine with only those modes which capture 90% of the average energy in the ensemble$U^i$, imposing condition that none of the neglected mode has more than 1% of the energy of the most energetic mode. For obtaining eigenfunctions the method of snapshots proposed by Sirovich [10] is applied to the data set obtained from thermal large eddy simulation of channel flow. In this work 3000 snapshots have taken. It is observed from nearly 2500 modes are required for full turbulent channel flow to capture 90% of the average energy at $R_\theta = 1$.

## 3.0 RESULTS AND DISCUSSION

After performing decomposition, snapshot independency test is being carried out for determining adequate number of snapshots which captures 90% of the total energy. This study is conducted for both the cases.

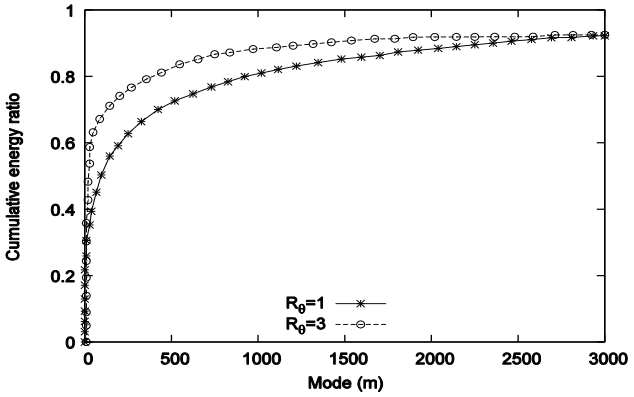


**Figure 1(a)** Cumulative energy ratio for $R_\theta = 1$ & $R_\theta = 3$ at $\mathrm{Re}_\tau = 180$

Figure 1(a) shows the cumulative energy ratio for the channel flow at $\mathrm{Re}_\tau = 180$. and for two values of temperature ratio $R_\theta$. It is observe that nearly 2500 modes are required for full turbulent channel flow to capture 90% of the average energy at $R_\theta = 1$.

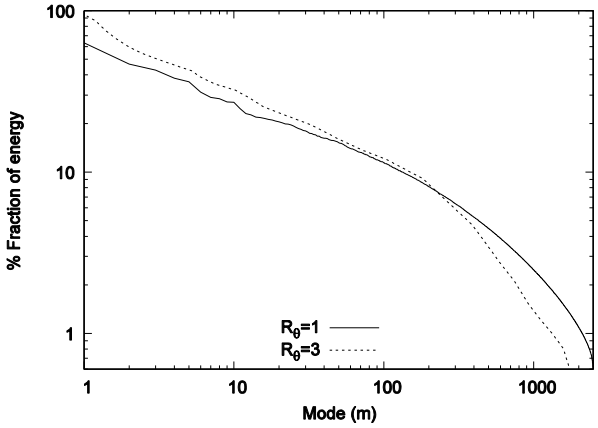


**Figure 1(b)** Eigenvalue spectra for $R_\theta = 1$ & $R_\theta = 3$ at $\mathrm{Re}_\tau = 180$

However with the strengthening of temperature stratification the initial sum of the energy in the lower modes increases and snapshot independency for 90% of average energy is being achieved at m = 2000. In Figure 1(b) eigen spectra is shown which gives an estimation of fractional energy ratio of eigenvalues w.r.t modes. It is obvious from Figure 1(a&b) that thermal stratification increase the relative energy content of the lower modes as compare to the simple channel flow with $R_\theta = 1$. The faster convergence of the second case can be attributed to local relaminarization at hot side of the domain [16], which typically reduces the scales of flow. The lower modes correspond to the larger scale, energy containing features of the flow, and the higher modes to the smaller scale, less energetic features of the flow. Therefore flow dynamics is best described by lower modes which contribute largely to the flow. In Table 1 individual contribution of KL mode to total energy and cumulative energy of turbulent fluctuation (kinetic energy plus scalar variance) of the first 20 most energetic modes are reported for both the cases. The first 20 modes obtained from method of snapshots for the case $R_\theta = 1$ alone contribute to 21.3% of the total energy whereas the contribution of first energetic mode is near about 3%. For the non-isothermal case at$R_\theta = 3$, the accountability of first 20 modes are more as compare to the plane channel flow, contributing about 29.5% of the total energy. Also the residing energy in the first most energetic modes for the case $R_\theta = 3$is higher than the case $R_\theta = 1$, exhibits about 6.2% of the total energy. In Figure 2. iso-surfaces of streamwise velocity uctuations at $R_\theta = 1$ reconstructed from 2350 POD modes obtained from decomposition is shown, which contributes about 90% of the total energy. It is observe that different flow structures are observed mainly in streamwise (light surfaces are positive while dark surfaces represents negative streamwise velocity) direction.

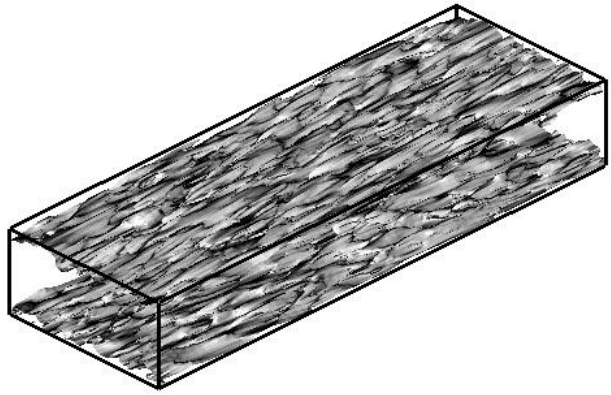

**Figure 2** Iso-surfaces of streamwise velocity fluctuation reconstructed from first most energetic 2350 POD modes

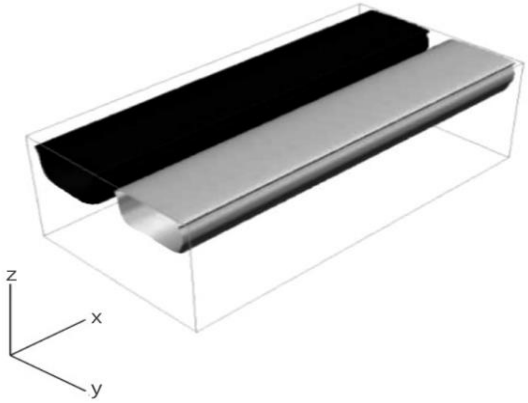


**Figure 3** Surfaces of constant streamwise velocity fluctuations reconstructed from first most energetic mode of POD at $R_\theta = 3$

**Table 1** Energy content of the first 20 POD eigenfunctions

| Mode | $R_\theta = 1$ | | $R_\theta = 3$ | |
|---|---|---|---|---|
| | Energy Fraction | Energy Sum | Energy Fraction | Energy Sum |
| 1 | 0.02920 | 0.02920 | 0.06275 | 0.06275 |
| 2 | 0.02010 | 0.04930 | 0.04452 | 0.10727 |
| 3 | 0.01535 | 0.05465 | 0.02210 | 0.12937 |
| 4 | 0.01405 | 0.06870 | 0.02052 | 0.14989 |
| 5 | 0.01340 | 0.08210 | 0.01632 | 0.16621 |
| 6 | 0.01191 | 0.09401 | 0.01353 | 0.17974 |
| 7 | 0.01155 | 0.10556 | 0.01250 | 0.18224 |
| 8 | 0.01095 | 0.11651 | 0.01112 | 0.19336 |
| 9 | 0.01011 | 0.12662 | 0.01095 | 0.20431 |
| 10 | 0.00995 | 0.13657 | 0.01005 | 0.21436 |
| 11 | 0.00915 | 0.14582 | 0.00990 | 0.22426 |
| 12 | 0.00890 | 0.15472 | 0.00905 | 0.23331 |
| 13 | 0.00851 | 0.16323 | 0.00875 | 0.24206 |
| 14 | 0.00835 | 0.17158 | 0.00850 | 0.25056 |
| 15 | 0.00805 | 0.17963 | 0.00815 | 0.25871 |
| 16 | 0.00795 | 0.18758 | 0.00802 | 0.26673 |
| 17 | 0.00750 | 0.19508 | 0.00785 | 0.27458 |
| 18 | 0.00709 | 0.20207 | 0.00747 | 0.28205 |
| 19 | 0.00680 | 0.20687 | 0.00703 | 0.28908 |
| 20 | 0.00655 | 0.21342 | 0.00690 | 0.29598 |

Iso-surfaces of Figure 2 did not bring about any physical interpretation about the flow dynamics in terms of energetic structures. These structures are obviously more difficult to identify. Therefore small scale effects are filtered out by considering individual contribution of lower number POD modes. To put more stress in detecting the energetic structures of thermally stratified flow, first five dominant modes are taken for plane turbulent channel flow as well as flow experiencing high thermal gradient. Iso-surfaces of streamwise velocity fluctuations are made. Non-isothermal flow have higher energy content in the first mode, contributing about 6.2% of the total energy shown in Figure 3.

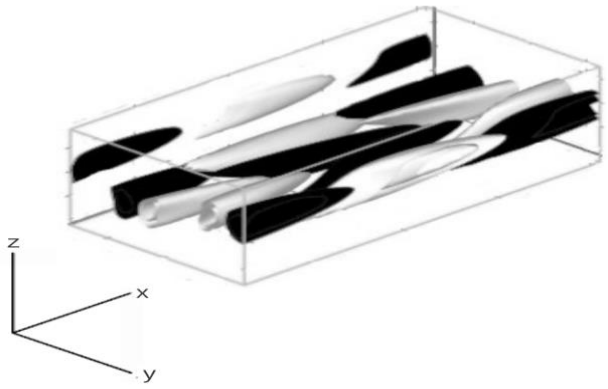


**Figure 4** Iso-surfaces of temperature fluctuations at $R_\theta = 3$. reconstructed from first most energetic mode of POD

Average flow structures are presented for the time interval 0 < t+ < 4000 (time for capturing m snapshots). The truncated shape of the flow structure owing to the contribution of thermo-fluid properties variation at high value of temperature ratio $R_\theta = 3$. These two patterns of dark (negative velocity) and light (positive velocity) surfaces are elongated in +x streamwise direction and have strong resemblance that of roll modes observed by Webber *et al*. [14] in minimal channel flow. It is clear from Figure 4, the dynamical structure for temperature variance of first mode is somewhat complex with merging of blunt shape pointed structures in a streamwise direction. We refer these modes as semi-roll modes for temperature fluctuation. In Figure 5 combined dynamical structure of first and second mode are presented which further enhanced the merging of semi-roll modes, indicating that temperature is violently torn up resulting in effective mixing with turbulent motions. Figure 6 describe the reconstruction made up of third most energetic mode for non-isothermal case showing bean shaped structure and accounts for 2.2% of the total energy. The structure shows couple of light and dark surfaces aligned in streamwise direction slightly tilted away from the wall. These structures are same as observed by Webber *et al*. [14], who gave the name of these modes as propagating mode shows an outward angle to be 30° from the wall. Similar structures have also been observed by Robinson [1] in his research

on coherent motions and named these structures as quasi-streamwise vortices tilted outward from the wall. Webber *et al*. [14] identified these modes as streamwise dependent and have fourfold degeneracy associated a plane wave with it moving obliquely from fow direction. On contrast to the minimal channel flow, non-isothermal case shows a modulation in structure due to temperature stratification but the overall flow behavior is same.

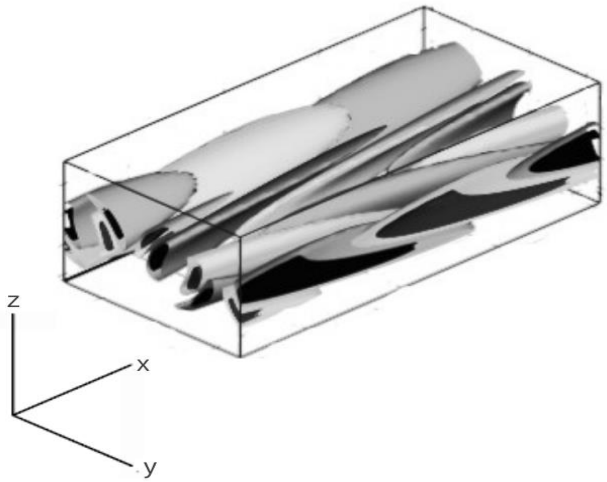


**Figure 5** Iso-surfaces of temperature fluctuations at $R_\theta = 3$. reconstructed from first + second mode of POD

### 3.1 Flow Dynamics

We now investigate how these structures are evolved during time which further gives us a detailed overview of flow dynamics. For this purpose total energy of the system is described in temporal coefficient form as [14]

$$E(t) = \sum_m a^m(t)a^{-m}(t) \qquad (3)$$

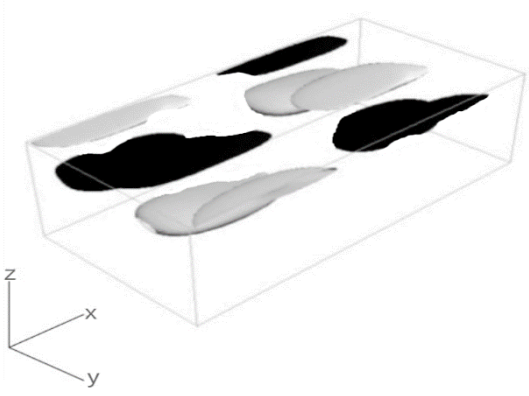


**Figure 6** Iso-surfaces of streamwise fluctuations at $R_\theta = 3$. reconstructed from third mode of POD

The portion of energy in any of the mode can be calculated as $p^m(t) = a^m(t)a^{-m}(t)/E(t)$, where $p^m(t)$ is a probability. Besides this a representational entropy [14] S(t) is also evaluated which measures the degree of distribution of energy over the modes given by

$$S(t) = -\sum_m p^m(t)\ln(p^m(t)) \qquad (4)$$

A small value of S(t) indicates that few modes contain the bulk of the energy while a large value of S(t) indicates that the energy is distributed over many modes. A plot of E(t) is shown in Figure 7 built by considering first 2350 modes for simple channel flow. Two high peaks are observed near time t+ = 420 and t+ = 1700 apart from some smaller spikes. In an interval 125 < t+ < 600 a sharp rise and then subsequent fall of energy occurs pointing towards the turbulent event.

Similar turbulent event also occur in an interval 1500 < t+ < 1900 with slightly lower peaks. These features are also observed by Webber *et al*. [14] in a minimal channel flow. To make study more fruitful distribution of representational entropy is also plotted for the same interval. The corresponding plot of S(t) (see Figure 8) shows a drop in its value to a lowest level where energy is high. This indicates that during the energy growth cycle, the energy is distributed over fewer modes and flow is well organized. After t+ = 410 entropy starts growing while energy is still high, indicates that the energy is redistributed over many modes in a small interval of time after which the energy decreases. This event describe the distribution of roll modes energy to propagating modes which break up the rolls into smaller scale structures, thereby increasing the energy of propagating modes. This breaking of well organized structure of rolls into smaller scale bean shaped modes termed as intermittent bursting phenomena.

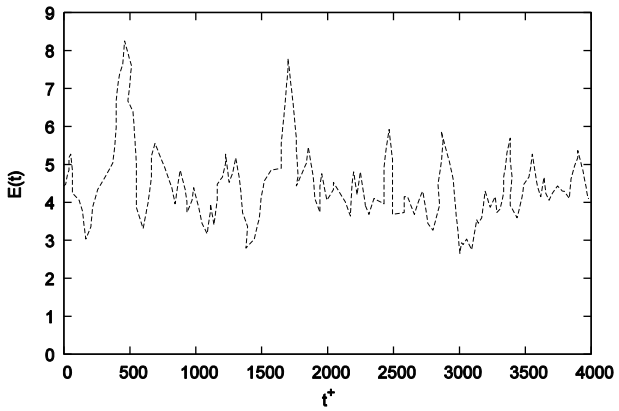


**Figure 7** Representation of time behavior of flow structure via total fluctuating energy for the first 2350 modes at $R_\theta = 1$

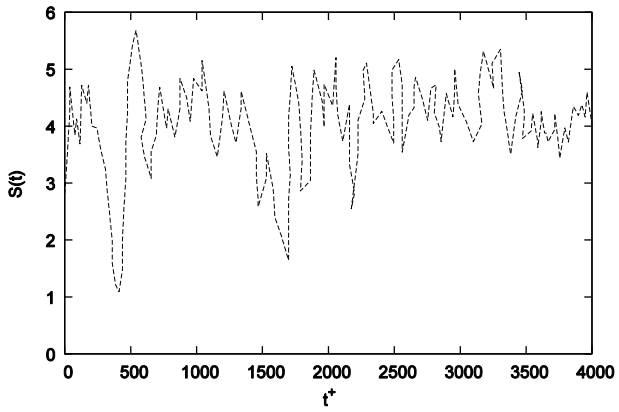


**Figure 8** Representation of time behavior of flow structure via entropy for the first 2350 modes at $R_\theta = 1$

In Figure 9 non-isothermal case is discuss for temporal behavior of flow structures. The plotted average energy E(t) as a function of non-dimensional time shows a constant level of fluctuating energy with one little peak at t+ = 1000, all other smaller spikes are showing constant fluctuations about mean line. This behavior at $R_\theta = 3$. qualitatively describe the role of temperature stratification which stabilizes the roll mode energy and prevent them from breakup into smaller scales (i.e the rate of bursting event decreases). The phenomena are observed near the hot wall of the domain, where viscosity is high due to high thermal gradient showing relaminarization [16]. This feature strengthens the lower number modes and depletion in the propagating modes resulting in modulation of quasi-streamwise vortices. It is already observed by Q criterion in the paper by Yahya *et al*. [16], that streaks formation ceases at the hot wall due to thermal stratification.

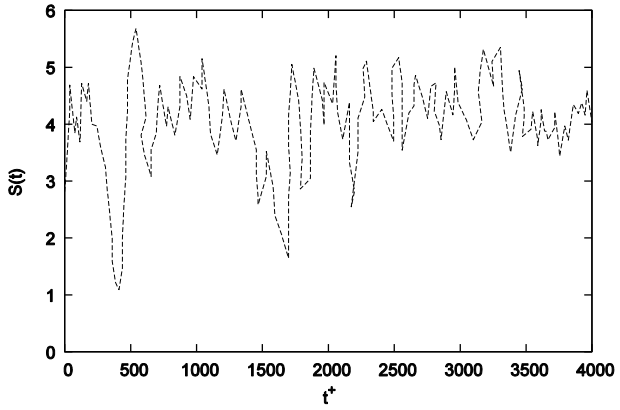


**Figure 9** Representation of time behavior of flow structure via total fluctuating energy for the first 2050 modes at $R_\theta = 3$

In Figure 10 entropy is shown which replicates the same behavior as of energy and no entropy event is shown which distribute the energy to many modes. The overall behavior is to build the energy in the roll modes and depletion in the bean-shaped mode. In contrast to the statement of Webber *et al*. [19] the roll size did not increase in non-isothermal case because the average fluctuating energy in this case is the sum of thermal and kinetic fields in which temperature advection tends to push the kinetic field during intense mixing and responsible for blunting of roll size.

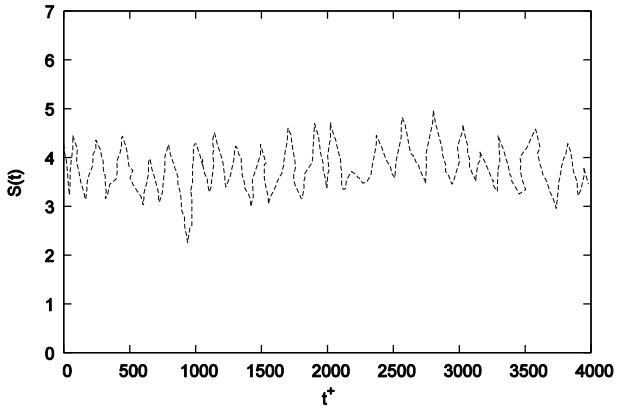


**Figure 10** Representation of time behavior of flow structure via entropy for the first 2050 modes at $R_\theta = 3$

Relaminarization occurs at the hot wall due tothe breaking in the mechanism of energy supplying from the roll modes to the propagating mode, this statement is in agreement with Duggleby *et al*. [20] that if any leg of the energy cycle in a turbulent flow is disrupted, the resulting imbalance can lead to the start of relaminarization process, and even complete relaminarization.

## 4.0 CONCLUSION

Information regarding the wall bounded turbulence subjected to high temperature gradient is carried out by performing proper orthogonal decomposition of a turbulent channel flow. A numerical database for thermal and kinetic fields is taken from previous study for educing modes. An extensive analysis is performed for the first five most energetic modes in order to describe the flow structure and its dynamic. In this study it is observed that the dominant structure are the roll modes which carries maximum proportion of energy aligned in streamwise direction. Same counterpart are also observed for thermal field and termed as semi-roll modes (because of their shape). Bean shaped modes are also evident from the structure of third mode for both the fields that are tilted little outward from the wall. Energy and entropy

plots describe the flow dynamics by giving an overview of triad interactionof streamwise elongated modes and quasi-streamwise modes which results in distribution of energy to large number of modes. However for non-isothermal case this breaking mechanism get slower, decreases the bursting rate and hence relaminarization is being observed on the hot wall.

## Acknowledgement

We are grateful for the HPC lab of Mechanical Engineering Department AMU for their generous support.

## References

[1] Robinson, S. K. 1991. Coherent Motions in the Turbulent Boundary Layer. *Annu. Rev. Fluid Mech*. 23: 601-639.
[2] Kasagi, N., Sumitani, Y., and Lida, O. 1995. Kinematics of the Quasi-coherent Vortical Structure in Near-wall Turbulence. *Int. J. Heat & Fluid Flow*. 16: 2-10.
[3] Kravchenko, A. G., Choi, H., and Moin, P. 1993. On the Relation of Near-wall Streamwise Vortices to Wall Skin Friction in Turbulent Boundary Layers. *Phys. Fluids A*. 12: 3307-3309.
[4] Kline, S. J., Reynolds, W. C., Schraub, F. A., and Runstadler, P. W. 1967. The Structure of Turbulent Boundary Layers. *J. Fluid Mech.* 30: 741-773.
[5] Hamilton, J. M., Kim J., and Waleffe, F. 1995. Regeneration Mechanisms of Near-wall Turbulence Structures. *J. Fluid Mech.* 287: 317-348.
[6] Perry, A. E., and Chong, M. S. 1991. A Description of Eddying Motions and flow Patterns Using Critical-point Concepts. *Annu. Rev. Fluid Mech*. 19: 125-155.
[7] Zhou, J., Adrian, R. J., Balachandar, S., and Kendall, T. M. 1999. Mechanisms for Generating Coherent Packets of Hairpin Vortices in Channel flow. *J. Fluid Mech.* 387: 353-396.
[8] Jeong, J. and Hussain, F. 1995. On the Definition of a Vortex. *J. Fluid Mech*. 285: 69-94.
[9] Lumley, J. L. 1971. *Stochastic Tools in Turbulence*. 1st ed. Academic Press, New York, NY.
[10] Sirovich, L. 1987. Turbulence and the Dynamics of Coherent Structures. Part I: Coherent Structures. Part II: Symmetries and Transformations. Part III: Dynamics and Scaling. *Q. Appl. Math*. 45: 561-590.
[11] Berkooz, G., Holmes, P., and Lumley, J. L. 1993. The Proper Orthogonal Decomposition in the Analysis of Turbulent flows. *Annu. Rev. Fluid Mech.* 25: 539-575.
[12] Sirovich, L., Kirby, M., and Winter, M. 1990. An Eigenfunction Approach to Large Scale Transitional Structures in Jet flow. *Phys. Fluids A*. 2: 127-136.
[13] Ball, K. S., Sirovich, L., and Keefe, L. R. 1991. Dynamical Eigenfunction Decomposition of Turbulent Channel Flow. *Int. J. Numer. Meth. Fluids*. 12: 585-604.
[14] Webber, G. A., Handler, R. A., and Sirovich, L. 1997. The Karhunen–Lo´Eve Decomposition of Minimal Channel Fow. *Phys. Fluids*. 9: 1054-1066.
[15] Jim´enez J. and Moin P. 1991. The Minimal FLow Unit in Near-wall Turbulence. *J. Fluid Mech*. 225: 213-240.
[16] Yahya, S. M., Anwer S. F., and Sanghi, S. 2013. Phenomenological and Statistical Analyses of Turbulence in Forced Convection with Temperature-Dependent Viscosity Under Non-Boussinesq Condition. *Eur. Phys. J. E*. 36: 120.
[17] Lumley, J. L., and Poje, A. 1997. Low-dimensional Models for flows with Density Fluctuations. *Phys. Fluids*. 9: 2023-2031.
[18] Deane, A. E., and Sirovich, L. 1991. A Computational Study of Rayleighbenard Convection. Part I. Rayleigh-number Scaling. *J. Fluid Mech.* 222: 231-250.
[19] Webber, G. A., Handler, R. A., and Sirovich, L. 2002. Energy Dynamics in a Turbulent Channel Flow using the Karhunen-Loeve Approach. I*nt. J. Numer. Meth. Fluids*. 40: 1381-1400.
[20] Duggleby, A., Ball, K. S., and Paul, M. R. 2007. Dynamics of Propagating Turbulent Pipe Flow Structures. Part II: Relaminarization. arXiv:physics/0608259 [physics.u-dyn] 0608: 1-20.